

Article

Trigonal Bipyramidal Rhodium(I) Methyl and Phenyl Complexes: Precursors of Oxidative Methyl and Phenyl Radical Generation

Urs Fischbach¹, Matthias Vogt² , Peter Coburger³, Monica Trincado^{3,*}  and Hansjörg Grützmacher^{3,*}¹ Cilag AG, 8200 Schaffhausen, Switzerland; ufischba@its.jnj.com² Institut für Chemie, Naturwissenschaftliche Fakultät II, Martin-Luther-Universität Halle-Wittenberg, Kurt-Mothes-Str. 2, 06120 Halle, Germany; matthias.vogt@chemie.uni-halle.de³ Department of Chemistry and Applied Biosciences, ETH Zürich, Vladimir-Prelog-Weg 1-5/10, 8093 Zürich, Switzerland; pcoburger@inorg.chem.ethz.ch

* Correspondence: trincado@inorg.chem.ethz.ch (M.T.); hgruetzmacher@ethz.ch (H.G.); Tel.: +41-44-633-48-15 (M.T.); +41-44-632-28-55 (H.G.); Fax: +41-44-633-10-31 (H.G.)

Abstract: The new complexes [Rh(Me)(trop₃P)] (**2**) and [Rh(Ph)(trop₃P)] (**3**) (trop = 5*H*-dibenzo[*a,d*]cyclohepten-5-yl) were synthesised by addition of organolithium reagents (MeLi and PhLi) to the parent pentacoordinated chloride complex [RhCl(trop₃P)]. The compounds have a trigonal bipyramidal structure with olefin-only ligands in the equatorial position and the methyl or phenyl substituent in the axial position. Oxidation of complexes **2** and **3** leads to the liberation of methyl and phenyl radicals, which were indirectly detected by reaction with common spin trapping reagents.

Keywords: rhodium; organic free radicals; alkyl complex; olefin ligands; homolysis Rh-C bond



Citation: Fischbach, U.; Vogt, M.; Coburger, P.; Trincado, M.; Grützmacher, H. Trigonal Bipyramidal Rhodium(I) Methyl and Phenyl Complexes: Precursors of Oxidative Methyl and Phenyl Radical Generation. *Inorganics* **2022**, *10*, 28. <https://doi.org/10.3390/inorganics10030028>

Academic Editor: Riccardo Peloso

Received: 7 February 2022

Accepted: 18 February 2022

Published: 24 February 2022

Publisher's Note: MDPI stays neutral with regard to jurisdictional claims in published maps and institutional affiliations.



Copyright: © 2022 by the authors. Licensee MDPI, Basel, Switzerland. This article is an open access article distributed under the terms and conditions of the Creative Commons Attribution (CC BY) license (<https://creativecommons.org/licenses/by/4.0/>).

1. Introduction

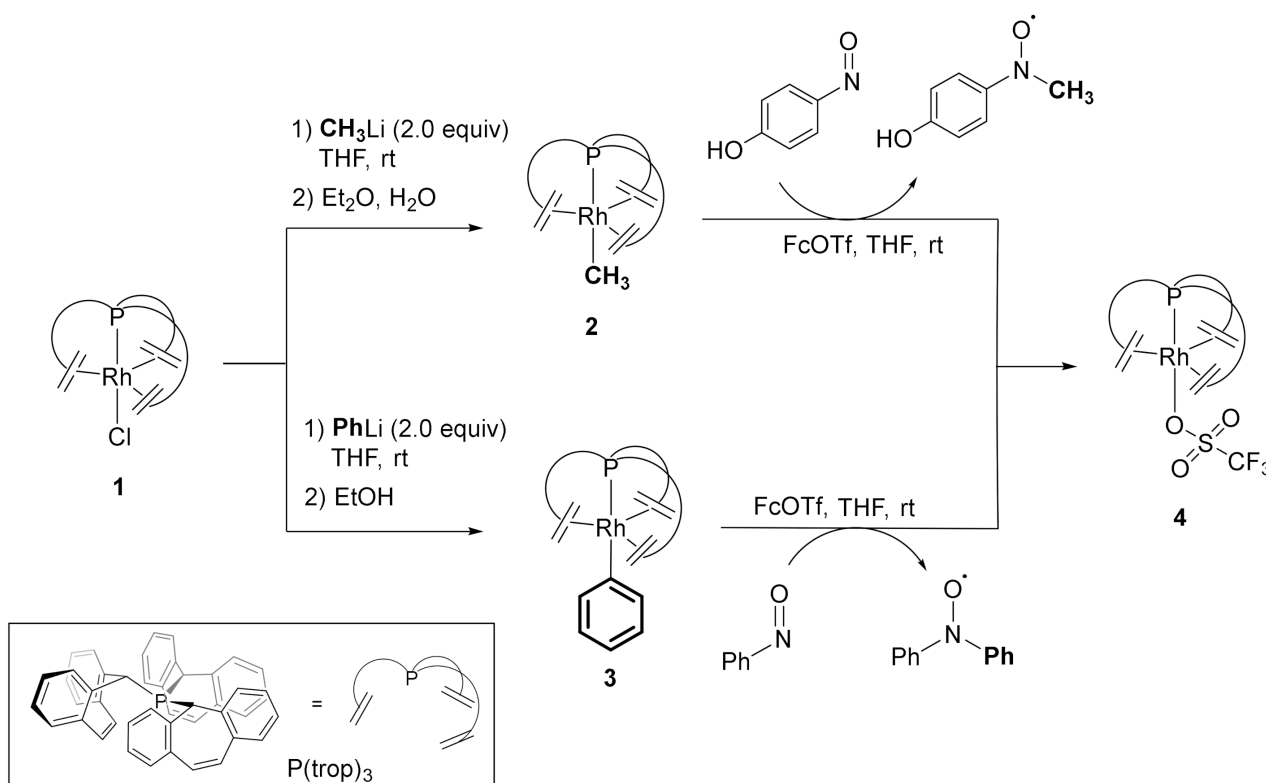
A large number of methods for the generation of C-centred radicals have been discovered in the past few years. The most relevant include thermolysis or photolysis of organic peroxides, azo, and carbonyl compounds [1–4]. Methyl radicals were observed for the first time by Kolbe in 1849 in the electrolysis of acetic acid [5]. Nowadays, the most important starting materials for the production of methyl radicals are acetyl peroxide and azomethane [6]. Common thermal sources of methyl radicals include (tBuO)₂, HgMe₂, CdMe₂, ZnMe₂, AsMe₃, SbMe₃, BiMe₃, AgMe, SiMe₄, SnMe₄, PbMe₄, SnCl₂Me₂, and CH₃CHO [1]. The photolytic generation is often reported to be favourable with respect to the thermal generation because of the more controllable and less drastic conditions. Another important method for the generation of methyl radicals in aqueous media is the reaction of sulphoxides with hydroxyl radicals, produced either by redox chemistry (Fenton), hydroperoxide photolysis, or pulse radiolysis [7–9]. Less common methods embrace photolysis of acetone, azoethane, HgMe₂, CH₃CHO, ketene, biacetyl, and MeI [10]. Methyl radicals decay extremely rapidly. In the gas or liquid phase, either by reaction with a second methyl radical forming ethane or by reaction with a molecule in the surrounding, e.g., a solvent molecule from which often hydrogen is abstracted. The stability of C-centred radicals can conveniently be expressed using the isodesmic H-transfer reaction: •CH₃ + R-H → CH₄ + •R. The reaction enthalpy of this process is commonly referred to as the radical stabilisation energy (RSE) of the newly formed radical relative to the unsubstituted methyl radical. For the unsubstituted phenyl radical, for example, an RSE value of +32.9 kJ mol⁻¹ has been determined (Ph-H BDE = 472.2 kJ mol⁻¹, H₃C-H BDE = 439.3 kJ mol⁻¹) [11], indicating that phenyl radicals are significantly less stable than alkyl radicals. This is simply due to the fact that the C–H bonds in benzene are significantly stronger than the primary C–H bonds in alkanes. The phenyl radical (•C₆H₅) has been shown to be a very important transient intermediate in the formation of polycyclic aromatic hydrocarbons (PAHs) and

soot in hydrocarbon combustion [12–14]. Therefore, it has been thoroughly characterised by UV, [15] IR, [16] and Raman spectroscopy [17]. The kinetics of its reactivity with various reagents (e.g., propene, [18] ketene, [19] methylacetylene, [20] or *n*-Bu₃SnH [21]) have been extensively studied. Various precursors can be chosen in order to obtain phenyl radicals such as benzoyl peroxides, [22–25] benzoic anhydride, [26] halogenobenzenes, [27] and nitrosobenzene [28,29]. Photodissociation of aryl halides in solution proved to be useful in chemical synthesis. Classical methods such as laser flash photolysis [30,31] or pulse radiolysis are the tools of choice for investigations of phenyl radicals [32]. The photodissociation of halobenzenes has been studied in molecular beams with femtosecond time resolution by pump–probe spectroscopy [33,34]. Another general approach for the generation of hydrocarbyl radicals is the irradiation of organometallic compounds. Soon after the structural elucidation of vitamin B₁₂ [35–37], it was found that cobalt–carbon bonds, in general, are prone to undergo homolysis under irradiation. This was confirmed for simple compounds such as [Co(dmgh)₂(CH₃)(H₂O)] (dmg = dimethylglyoxime) and [Co(CH₃)([14]aneN₄)(H₂O)](ClO₄)₂ ([14]aneN₄ = 1,4,8,11-tetraazacyclotetradecane), which can be used as a source for methyl radicals in kinetic investigations [38]. Homolytic fission of the Rh–CH₃ bond was observed in the electrochemical one-electron reduction of [Rh^{III}(η⁵-C₉H₇)(CH₃)(dppp^{*})]BPh₄ (dppp^{*} = Ph₂PCH(CH₃)CH₂PPh₂) in acetonitrile, which produced [Rh(η⁵-C₉H₇)(dppp^{*})] [39]. In a different report, the reaction of the paramagnetic Rh^{II} compound [Rh(2,4,6-*i*Pr₃C₆H₂)₂(tht)₂] (tht = tetrahydrothiophene) with *t*BuNC in *d*₈-toluene yielded [Rh{*t*BuN=C-(2,4,6-*i*Pr₃C₆H₂)}(*t*BuNC)₃] and monodeuterated triisopropylbenzene as a result of a deuterium abstraction reaction by the formed aryl radical from the solvent [40]. Electrolysis of Vaska type organometallic complexes as [Ir(CH₃)(CO)(PPh₃)₂] in 1,2-dichloroethane in presence of excess PPh₃ yielded [Ir(CO)(PPh₃)₃]⁺, [IrCl(CO)(PPh₃)₂] and methane [41]. This outcome suggests that the formed *d*⁷ species undergo radical dissociation, followed by a fast reaction of the formed •CH₃ with the solvent. For dialkyl Pd^{II} and Pt^{II} complexes, the oxidative cleavage of hydrocarbyl radicals upon one-electron oxidation is commonly observed [42]. Nevertheless, none of the aforementioned methods has ever been used for the quantitative and controlled release of methyl or phenyl radicals and for their application in sequential chemical transformations.

Recently, we established the synthesis of the new bulky ligand trop₃P (tris(5H-dibenzo [a,d]cyclohepten-5-yl)phosphane) and transition metal complexes thereof [43]. The Rh–P bond in complexes such as [RhCl(trop₃P)] (1) proved to be especially strong and, therefore, exhibited a large trans-influence on the opposing axial ligands. In preliminary investigations, we found that the diphenylphosphinyl compound [Rh(PPh₂)(trop₃P)] can easily be oxidised by FcOTf to give the pentacoordinated complex [Rh(OTf)(trop₃P)] and a •PPh₂ radical [44]. The in situ formation of diphenylphosphinyl radicals was evidenced by spin trapping reactions. Herein, we report the synthesis of the organometallic methyl and phenyl analogous compounds [Rh(Me)(trop₃P)] (2) and [Rh(Ph)(trop₃P)] (3). The oxidation of these complexes gives rise to the controlled release of methyl or phenyl radicals, respectively.

2. Results and Discussion

The addition of two equivalents of MeLi to the complex [RhCl(trop₃P)] ((1) resulted in a fast colour change from the suspended yellow starting material to an intensely deep green solution. This solution was quenched with a small amount of water (Et₂O containing traces of water) to give the methyl complex [Rh(CH₃)(trop₃P)] (2) (Scheme 1). The use of exactly two equivalents of MeLi was crucial to obtain a quantitative yield of the final product. Compound 2 is remarkably stable to air and moisture at room temperature; however, heating the product in the presence of water or alcohol solvents resulted in decomposition and elimination of methane.



Scheme 1. Synthesis of methyl and phenyl rhodium(I) complexes **2** and **3** and their reactivity upon oxidation. (FcOTf = ferrocenyl triflate).

Complex **2** was fully characterised by spectroscopic methods (see ESI for details). The ^1H NMR spectrum shows one resonance at $\delta = -1.01$ ppm, which is attributed to the methyl group coordinated to rhodium and displays coupling to both nuclei, ^{31}P ($^3J_{\text{PH}} = 5.6$ Hz) and ^{103}Rh ($^2J_{\text{RH}} = 1.1$ Hz). The large ^{13}C ^{31}P coupling, $^2J_{\text{PC}} = 114$ Hz, in the ^{13}C NMR spectrum indicated a *trans*-position of both nuclei within the trigonal pyramidal coordination sphere. All benzylic and olefinic protons are in magnetically equivalent positions, which is in accord with the proposed C_{3v} symmetric structure. Single crystals of the compound were grown by layering a toluene solution of the complex with *n*-hexane and investigated using X-ray diffraction methods. Unfortunately, we failed to obtain a dataset which allows discussing the molecular structure of complex **2** in detail, but the overall connectivity and form could be determined (Figure 1a; see also Table S1 in Supplementary Materials). The methyl group resides in an axial position oriented *trans* to the P atom of the trop_3P ligand. This feature is remarkable in the realm of $\text{Rh}^{\text{I}}\text{-CH}_3$ complexes. Very few crystal structures of $\text{Rh}^{\text{I}}\text{-CH}_3$ species have been reported. The most similar structure is $[\text{Rh}(\text{CH}_3)(\text{CO})\{\kappa^3\text{-H}_3\text{CC}(\text{CH}_2\text{PPh}_2)_3\}]$, [45] where the methyl group is also coordinated *trans* to a phosphane ligand and the complex exhibits trigonal bipyramidal geometry. Other structures with a $\text{Rh}\text{-Me}$ unit show the more common square planar coordination sphere [46] or dimeric structures [47–49]. Following a similar synthetic route, the synthesis of complex $[\text{Rh}(\text{Ph})(\text{trop}_3\text{P})]$ (**3**) was performed using an excess of PhLi (2.0 equiv) in the reaction with complex **1** (Scheme 1). The initial orange suspension turned rapidly into a deep-green solution. The reaction mixture was subsequently quenched with ethanol, forming compound **3**. The NMR spectra of the product indicate high symmetry and confirm the formation of a pentacoordinated complex bearing the phenyl group in the axial position and the tris(olefinic) phosphine ligand in the three equatorial (olefins) and remaining axial position (phosphorus). The low-frequency ^{13}C NMR and ^1H NMR chemical shifts (5.85 and 75.8 ppm, respectively) of the coordinated olefin units, compared with the free trop_3P ligand, indicate substantial metal-to-olefin electron back-bonding which strengthens the $\text{Rh}\text{-}$

olefin bonds. The NMR signal to the *ipso*-carbon nucleus of the phenyl ligand bound to Rh was observed at 166.8 ppm (in the range of previously reported Ph–Rh^I complexes) [46,50], exhibiting the expected splitting due to coupling to both ¹⁰³Rh (¹J_{RhC} = 20 Hz) and to ³¹P (²J_{PC} = 114 Hz) in *trans*-position.

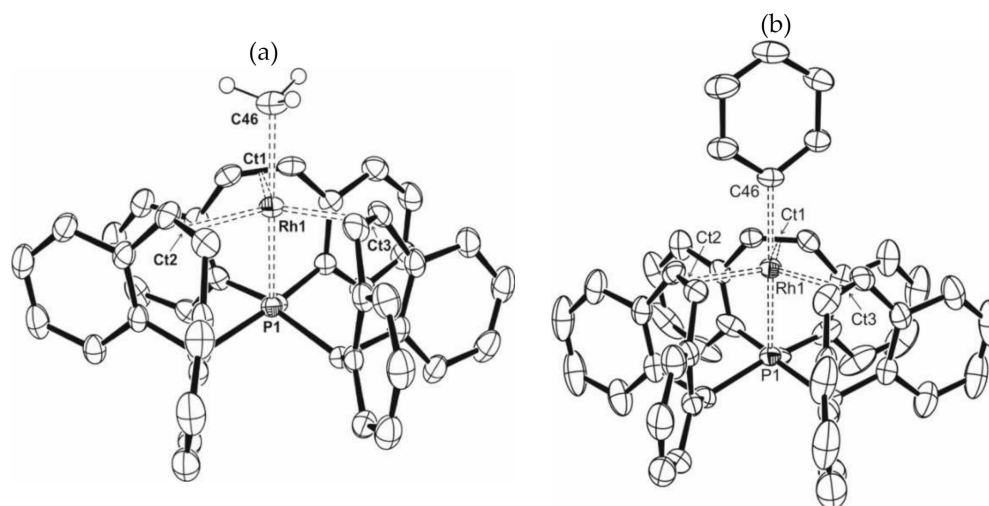


Figure 1. (a) Molecular structure of $[\text{Rh}(\text{CH}_3)(\text{trop}_3\text{P})] \times (0.5 \text{ C}_7\text{H}_8)$ (2). Hydrogen atoms and solvent molecules (toluene) are omitted for clarity; (b) ORTEP plot of $[\text{Rh}(\text{Ph})(\text{trop}_3\text{P})] \times (1.5 \text{ C}_7\text{H}_8)$ (3). Hydrogen atoms, phenyl substituent splitting, and toluene molecules were omitted for clarity. Thermal ellipsoids at 50% probability; selected bond lengths (Å) and angles (°): Rh1–P1: 2.2099(7); Rh1–C46: 2.149(3); P1–Rh1–C46: 178.37(8); $\Sigma^\circ \text{P1}$ 318.2.

Extraction with toluene and slow evaporation yielded yellow crystals of the complex, suitable for an X-ray diffraction analysis. The molecular structure of 3 is presented in Figure 1b (crystal data and structural refinement details can be found in Table S2 in Supplementary Materials).

Likewise, complex $[\text{Rh}(\text{Ph})(\text{trop}_3\text{P})] \times (1.5 \text{ C}_7\text{H}_8)$ (3) has an uncommon structure. As compound 2, complex 3 is a pentacoordinated complex with the double bonds of the trop_3P ligand arranged in the equatorial plane in an almost perfect coplanar fashion. According to Addison's τ_5 criterion [51], the coordination environment around the central atom can be described practically as an ideal trigonal bipyramid for both complexes ($\tau_5 = 1.01$ (2) and 0.96 (3)), with the phosphorous atom and alkyl ligands located in axial positions. The only comparable compounds reported previously are the square planar rhodium(I) complexes $[\text{Rh}(\text{Ph})(\text{PMe}_3)_3]$ [52] and $[\text{Rh}(\text{Ph})(\text{PMe}_3)_2(\text{CO})]$ [46], where the phenyl group is located *trans* to a triphenylphosphane or a carbonyl ligand, respectively. Another loosely related example is the dimeric complex $[\text{Rh}_2(\text{Ph})_2(\mu^2\text{-CO})(\kappa^2\text{-dppm})_2]$ [50], having an 'A-frame' type structure and including a Rh–Rh bond. Table 1 lists some selected crystallographic data of these compounds. Noteworthy is the long bond between the Rh centre to the *ipso*-C atom of the phenyl substituent (2.149(3) Å), when compared with previously reported Rh^I phenyl complexes (Table 1), which indicates a weakened Rh–C bond.

Table 1. Comparison of crystallographic data of Rh^I phenyl complexes.

Compound	Bond Length Rh–C _{<i>ipso</i>}	Bond Angle (<i>trans</i>)	[Ref]
3	2.149(3) Å	P–Rh–C 178.37(8)°	this study
$[\text{Rh}(\text{Ph})(\text{PMe}_3)_3]$	2.079(4) Å	P–Rh–C 170.0(1)°	[52]
$[\text{Rh}(\text{Ph})(\text{PMe}_3)_2(\text{CO})]$	2.096(4) Å	C–Rh–C 180°	[46]
$[\text{Rh}_2(\text{Ph})_2(\mu^2\text{-CO})(\kappa^2\text{-dppm})_2]$	2.066(5); 2.072(5) Å	Rh–Rh–C 166.4(1)°	[50]

The rhodium methyl compound **2** rapidly reacted with one equivalent of FcOTf. The $^{31}\text{P}\{^1\text{H}\}$ NMR spectrum shows the known rhodium complex $[\text{Rh}(\text{OTf})(\text{trop}_3\text{P})]$ (**4**) as the only phosphorus-containing oxidation product [44]. This observation indicates that the other product of the irreversible oxidation might be a methyl radical acting as a reactive intermediate. This hypothesis was corroborated by carrying out the oxidation reaction in the presence of TEMPO (2,2,6,6-tetramethyl-1-piperidinyloxy radical), which is a known radical trap and should lead to the formation of TEMPO–Me [53]. Indeed, TEMPO–Me was detected by both ^1H NMR spectroscopy and GC–MS. In a further experiment, the methyl radicals released upon oxidation of **2** were trapped with nitrosophenol which yielded the paramagnetic compound $\text{HO-C}_6\text{H}_4\text{-N}(\text{O}^\bullet)\text{CH}_3$. This compound could easily be detected by EPR spectroscopy. Additionally, indeed, an EPR spectrum was obtained which is characteristic for a radical with one large nitrogen coupling and three large proton couplings, which stem from the methyl group. The obtained radical $\text{HO-C}_6\text{H}_4\text{-N}(\text{O}^\bullet)\text{CH}_3$ has not been described in the literature, to the best of our knowledge, but the closely related anisole derivative $\text{H}_2\text{N-C}_6\text{H}_4\text{-N}(\text{O}^\bullet)\text{CH}_3$ has been reported, and the coupling constants are comparable (Figure 2) [54].

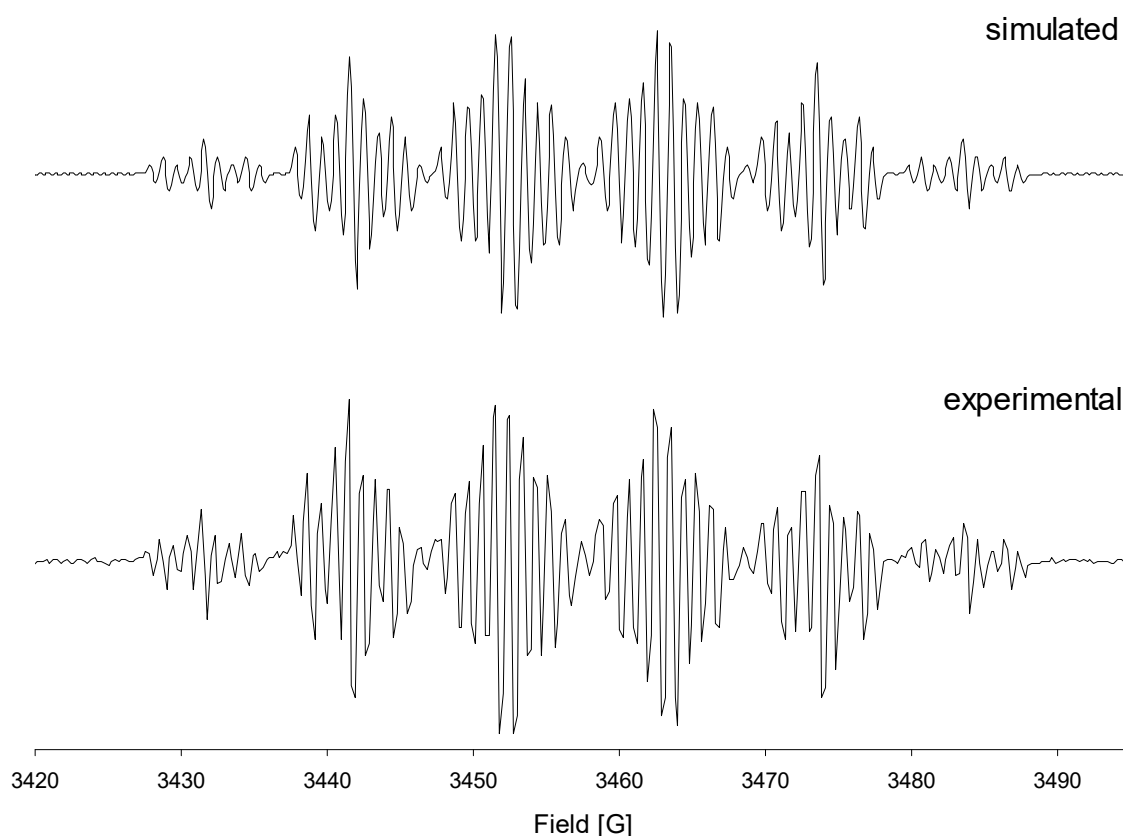


Figure 2. EPR spectrum of the spin trap adduct $\text{HO-C}_6\text{H}_4\text{-N}(\text{O}^\bullet)\text{CH}_3$, generated in the reaction of complex **2** with $p\text{-HO-C}_6\text{H}_4\text{-N=O}$ in the presence of FcOTf in THF. Top: simulated spectrum, bottom: experimental spectrum. Frequency: 9.727 GHz; g-value (vs. DPPH): 2.0044; hyperfine coupling constants: a_{N} : 30.9 MHz, $a_{\text{H,methyl}}$: 27.9 MHz, $a_{\text{H,ortho}}$: 7.9 MHz, $a_{\text{H,meta}}$: 2.6 MHz.

The reaction of **3** with FcOTf was much slower than with the methyl complex **2**, and complete conversion was achieved only after ca. 30 min. In analogy to the oxidation process observed for the methyl analogue, the organometallic product of this oxidation was the same complex **4**, observed spectroscopically. In order to show that oxidation of the phenyl complex leads to the production of phenyl radicals, we used in situ the spin trap nitrosobenzene, Ph-N=O . When the oxidation with FcOTf was carried out, an intense

and nicely resolved EPR spectrum of the spin trap adduct $\text{Ph}_2\text{N-O}^\bullet$ was observed by EPR spectroscopy (Figure 3), which is in agreement with the literature data [55].

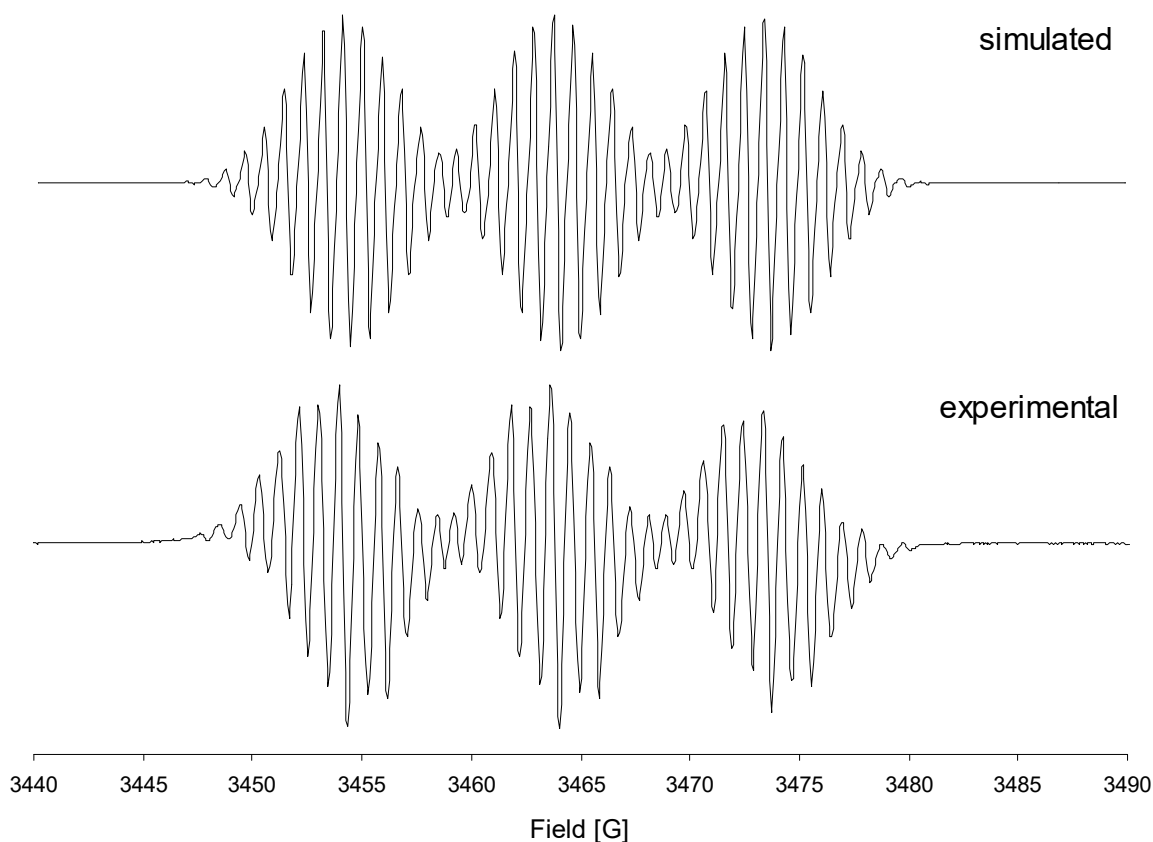
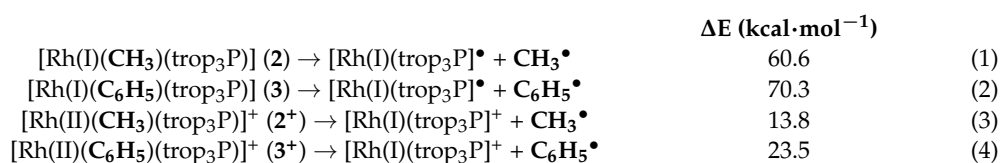


Figure 3. EPR spectrum of $\text{Ph}_2\text{N-O}^\bullet$, generated in the reaction of complex **3** and Ph-N=O in the presence of FcOTf in THF. Top: simulated spectrum, bottom: experimental spectrum. Frequency: 9.746 GHz; g-value (*vs.* DPPH): 2.0047; hyperfine coupling constants: a_{N} : 27.1 MHz, $a_{\text{H,ortho/para}}$: 5.1 MHz, $a_{\text{H,meta}}$: 2.5 MHz.

DFT methods were used in order to calculate the energy required to dissociate the Rh–C bond (methyl or phenyl ligand) from either the neutral d^8 -valence electron configured Rh^{I} complexes **2** or **3** (Equations (1) and (2)) or the d^7 -valence electron configured Rh^{II} complexes 2^+ or 3^+ , respectively, which are the products of the one-electron oxidation (Equations (3) and (4)). As expected, the Rh–C bond in the Rh^{I} phenyl complex **3** was about 16% stronger than in the methyl complex **2** and, in both dissociations, was endothermic by more than 60 kcal mol^{-1} , making these compounds stable under the experimental conditions. This dramatically changed upon oxidation, whereby the bond energy in **2** diminished by about 75% in 2^+ (13.8 kcal mol^{-1}) and 67% in 3^+ (23.5 kcal mol^{-1}). Nevertheless, the significantly higher calculated dissociation energy in 3^+ is consistent with the experimentally observed much slower decay of this complex in comparison with 2^+ .



In summary, facile synthesis of the new Rh^{I} methyl and phenyl compounds $[\text{Rh}(\text{R})(\text{trop}_3\text{P})]$ was accomplished. The trigonal pyramidal arrangement of the ligands with the organic substituent in axial position is unprecedented for d^8 Rh^{I} compounds. The complexes $[\text{Rh}(\text{R})(\text{trop}_3\text{P})]$ (**2**: R = Me; **3**: R = Ph) reacted with FcOTf to give the $[\text{Rh}(\text{trop}_3\text{P})]^+$

cation and methyl or phenyl radicals, indicating that the one-electron oxidation product $[\text{Rh}^{\text{II}}\text{R}(\text{trop}_3\text{P})]^+$ (R = Me, Ph) was unstable and decomposed under homolysis of the Rh–C bond. The formation of the radicals R^\cdot was evidenced by reactions with either a persistent radical to give a diamagnetic radical combination product or with spin trap reagents which gave persistent radicals as products that could be easily detected by EPR spectroscopy. To the best of our knowledge, this is the first time that methyl or phenyl radicals could be generated oxidatively from the corresponding alkyl and aryl metal complexes. This reactivity of **2** and **3** is similar to the one previously reported for the phosphinyl complex $[\text{Rh}(\text{PPh}_2)(\text{trop}_3\text{P})]$. We attribute this reactivity to the formation of the very stable and chemically inert complex $[\text{Rh}(\text{trop}_3\text{P})(\text{OTf})]$ and the special property of the phosphane ligand trop_3P whose phosphorus centre seemingly exercises a strong trans-influence and trans-effect on the trans bound ligand, especially in the Rh^{II} complexes which are the likely reactive intermediates. Based on the calculated Rh–C bond dissociation enthalpies, the formation of alkyl and aryl radicals from cationic Rh^{II} intermediates are rather favourable. The homolytic bond cleavage is easier for methyl than for the phenyl derivative, according to the DFT predictions and experimental observations. This eventually opens the possibility to use metal complexes of the general formula $[\text{MX}(\text{trop}_3\text{P})]$ as sources for X^\cdot radicals which we currently explore in our laboratory.

3. Materials and Methods

General methods and Supplementary Materials are available online, including spectroscopic data for complexes **2** and **3** and crystallographic data for **3**.

Data collection for the X-ray structure determinations was performed on a Bruker SMART 1K platform with graphite-monochromated Mo– $\text{K}\alpha$ radiation ($\lambda = 0.71073 \text{ \AA}$). The reflex intensities were measured by CCD area detectors. The collected frames were processed with the proprietary software SAINT, and an absorption correction was applied (SADABS). Solution and refinement of the structures were performed with SHELXS-97 and SHELXL-97, respectively. All non-hydrogen atoms were refined with anisotropic displacement parameters. Hydrogen atoms were placed in their idealised positions and were allowed to ride on the respective carbon atoms. CCDC 631208 contains the supplementary crystallographic data for **3**. These data can be obtained free of charge from The Cambridge Crystallographic Data Centre via www.ccdc.cam.ac.uk/data_request/cif (accessed on 31 January 2022)

DFT calculations were carried out with the ORCA program package [56]. Unless stated otherwise, all calculations were carried out on isolated molecules. Density fitting techniques, also called resolution-of-identity approximation (RI) [57], were used for GGA and *meta*-GGA calculations, and the RIJCOSX [58] approximation was used for hybrid-GGA and CASSCF calculations. Atom-pairwise dispersion corrections with the Becke–Johnson damping (D3BJ) [59,60] were used for all DFT calculations (D3(0) in case of M06). All geometries were obtained using the B97-3c method developed by the Grimme group [61]. Final energy calculations were performed using the M06 [62] functional, the def2-TZVPP [63] basis set, and the CPCM [64] model for THF.

Complex 2. Complex $\text{RhCl}(\text{trop}_3\text{P})$ **1** (260 mg, 0.35 mmol, 1.0 equiv) was suspended in dry THF (25 mL) and cooled in an ice bath. A solution of MeLi in Et_2O (1.6 M, 0.45 mL, 0.72 mmol, 2.0 equiv) was added dropwise until all the solids had dissolved. The colour of the resulting solution changed from light yellow to a strong dark green. Conversion of the reaction was checked by ^{31}P NMR spectroscopy. Et_2O (1.5 mL 1% *v/v* water) was added carefully to the reaction mixture provoking an immediate colour change to light yellow. The resulting solution was concentrated to dryness and extracted with CH_2Cl_2 ($2 \times 25 \text{ mL}$) to remove residual salts. The solution was concentrated, and the residue was extracted with hexane ($3 \times 50 \text{ mL}$). The combined extractions were concentrated to dryness and recrystallised from Et_2O . The precipitated product was collected by filtration, washed with Et_2O ($2 \times 3 \text{ mL}$), hexane ($2 \times 3 \text{ mL}$), and pentane ($2 \times 3 \text{ mL}$), and then dried in a

high vacuum. The obtained product was a microcrystalline light yellow powder. Yield: 95 mg (38%).

Complex 3. Complex [RhCl(trop₃P)] (1 (214 mg, 0.29 mmol, 1.0 equiv) was suspended in dry THF (15 mL) and a solution of PhLi in dibutyl ether (2.0 M, 0.29 mL 0.58 mmol, 2.0 equiv) was added dropwise. Upon addition, the suspended starting material dissolved, and the colour of the solution changed from light yellow to a strong dark green. Ethanol (50 µL) was added to the dark green solution, provoking an immediate colour change to orange. The solution was concentrated to dryness, and the residue was extracted with dry toluene (2 × 15 mL). The toluene solution was concentrated to ca. 5 mL and cooled to −18 °C. After 16 h, the precipitated product was collected by filtration and washed with diethyl ether (2 × 5 mL). After drying under high vacuum, complex 3 was isolated as a yellow crystalline powder. Yield: 127 mg (56%).

Supplementary Materials: The supporting information can be downloaded at: <https://www.mdpi.com/article/10.3390/inorganics10030028/s1>, including spectroscopic and crystal data of complexes 2 and 3.

Author Contributions: Conceptualization, U.F., M.T. and H.G.; methodology, U.F.; validation, M.V., P.C. and M.T.; formal analysis, M.V. and P.C. and M.T.; investigation, U.F. and M.T.; writing—original draft preparation, U.F.; writing—review and editing, M.T. and H.G.; supervision, M.T. and H.G.; project administration, H.G.; funding acquisition, H.G. All authors have read and agreed to the published version of the manuscript.

Funding: This research was funded by ETHZ (Eidgenössische Technische Hochschule Zürich; grant 0-20214-16) and the SNF (Schweizerischer Nationalfonds; grant 2-77199-18).

Institutional Review Board Statement: Not applicable.

Informed Consent Statement: Not applicable.

Data Availability Statement: Spectroscopic and crystal data are given in the supporting information. Crystallographic data can be obtained free of charge from the Cambridge Crystallographic Data Centre.

Acknowledgments: We thank W. Koppenol as well as R. Kissner for the supply and support of EPR instrumentation.

Conflicts of Interest: The authors declare no conflict of interest.

References

1. Gibian, M.J.; Corley, R.C. Organic radical-radical reactions. Disproportionation vs. combination. *Chem. Rev.* **1973**, *73*, 441–464. [[CrossRef](#)]
2. Leffler, J.E. *An Introduction to Free Radicals*; John Wiley & Sons, Inc.: New York, NY, USA, 1993.
3. Forbes, M.D.E. *Carbon-Centered Free Radicals and Radical Cations: Structure, Reactivity, and Dynamics*; John Wiley & Sons, Inc.: New York, NY, USA, 2010.
4. Fagnoni, M.; Ravelli, D.; Protti, S. *Generation of Carbon-Centered Radicals by Photochemical Methods*; Georg Thieme Verlag: Stuttgart, Germany, 2021.
5. Kolbe, H. Untersuchungen über die Elektrolyse organischer Verbindungen. *Liebigs Ann. Der Chem. Und Pharm.* **1849**, *69*, 257–274. [[CrossRef](#)]
6. Fossey, J.; Lefort, D.; Sorba, J. *Free Radicals in Organic Chemistry*; John Wiley & Sons: Chichester, UK, 1995.
7. Dixon, W.T.; Norman, R.O.C.; Buley, A.L. Electron spin resonance studies of oxidation. Part II.1 aliphatic acids and substituted acids. *J. Chem. Soc.* **1964**, 3621–3625. [[CrossRef](#)]
8. Lagercranz, C.; Forshult, S. Trapping of short-lived free radicals as nitroxide radicals detectable by ESR spectroscopy. The radicals formed in the reaction between OH-radicals and some sulphoxides and sulphones. *Acta Chem. Scand.* **1969**, *23*, 811–817. [[CrossRef](#)]
9. Dorfmann, L.M.; Sauer, M.C., Jr. *Investigation of Rates and Mechanisms of Reactions, Part II: Investigation of Elementary Reaction Steps in Solution and Fast Reaction Techniques*; Bernasconi, C.F., Ed.; Wiley-Interscience: New York, NY, USA, 1986.
10. Gray, P.; Herod, A.A.; Jones, A. Kinetic data for hydrogen and deuterium atom abstraction by methyl and trifluoromethyl radicals in the gaseous phase. *Chem. Rev.* **1971**, *71*, 247–294. [[CrossRef](#)]
11. Hioe, J.; Zipse, H. Radical stability and its role in synthesis and catalysis. *Org. Biomol. Chem.* **2010**, *8*, 3609–3617. [[CrossRef](#)]
12. Haynes, D.S. *Fossil Fuel Combustion*; Wiley-Interscience: New York, NY, USA, 1991; p. 261.

13. Bockhorn, H. *Soot Formation in Combustion*; Springer: New York, NY, USA, 1993.
14. Glassmann, I. *Combustion*, 2nd ed.; Academic Press: New York, NY, USA, 1986.
15. Engert, J.M.; Dick, B. The UV absorption spectrum of the phenyl radical isolated in solid argon. *Appl. Phys. B-Lasers Opt.* **1996**, *63*, 531–535. [[CrossRef](#)]
16. Friderichsen, A.V.; Radziszewski, J.G.; Nimlos, M.R.; Winter, P.R.; Dayton, D.C.; David, D.E.; Ellison, G.B. The infrared spectrum of the Matrix-isolated phenyl radical. *J. Am. Chem. Soc.* **2001**, *123*, 1977–1988. [[CrossRef](#)]
17. Lapinski, A.; Spanget-Larsen, J.; Langgard, M.; Waluk, J.; Radziszewski, J.G. Raman spectrum of the phenyl radical. *J. Phys. Chem. A* **2001**, *105*, 10520–10524. [[CrossRef](#)]
18. Park, J.; Nam, G.J.; Tokmakov, I.V.; Lin, M.C. Experimental and theoretical studies of the phenyl radical reaction with propene. *J. Phys. Chem. A* **2006**, *110*, 8729–8735. [[CrossRef](#)]
19. Choi, Y.M.; Lin, M.C. Kinetics and mechanisms for the reactions of phenyl radical with ketene and its deuterated isotopomer: An experimental and theoretical study. *ChemPhysChem* **2004**, *5*, 225–232. [[CrossRef](#)] [[PubMed](#)]
20. Kaiser, R.I.; Asvany, O.; Lee, Y.T.; Bettinger, H.F.; Schleyer, P.V.; Schaefer, H.F. Crossed beam reaction of phenyl radicals with unsaturated hydrocarbon molecules. I. Chemical dynamics of phenylmethylacetylene ($C_6H_5CCCH_3; X1A'$) formation from reaction of $C_6H_5(X2A1)$ with methylacetylene, $CH^3CCH(X1A1)$. *J. Chem. Phys.* **2000**, *112*, 4994–4999. [[CrossRef](#)]
21. Garden, S.J.; Avila, D.V.; Beckwith, A.L.J.; Bowry, V.W.; Ingold, K.U.; Luszyk, J. Absolute rate constant for the reaction of aryl radicals with tri-n-butyltin hydride. *J. Org. Chem.* **1996**, *61*, 805–809. [[CrossRef](#)] [[PubMed](#)]
22. Pacansky, J.; Bargon, J. Low temperature photochemical studies on acetyl benzoyl peroxide. the observation of methyl and phenyl radicals by matrix isolation infrared spectroscopy. *J. Am. Chem. Soc.* **1975**, *97*, 6896–6897. [[CrossRef](#)]
23. Pacansky, J.; Gardini, G.P.; Bargon, J. Low temperature studies on propionyl benzoyl peroxide and propionyl peroxide. The ethyl radical. *J. Am. Chem. Soc.* **1976**, *98*, 2665–2666. [[CrossRef](#)]
24. Pacansky, J.; Brown, D.W. Photolysis of acetyl benzoyl peroxide isolated in an argon matrix: The stability of the benzoyloxy and acetoxy radicals toward decarboxylation. *J. Phys. Chem.* **1983**, *87*, 1553–1559. [[CrossRef](#)]
25. Jacox, M.E. Reaction of F atoms with C_6H_6 . Vibrational spectrum of the C_6H_6F intermediate trapped in solid argon. *J. Phys. Chem.* **1982**, *86*, 670–675. [[CrossRef](#)]
26. Radziszewski, J.G.; Nimlos, M.R.; Winter, P.R.; Ellison, G.B. Infrared absorption spectroscopy of the phenyl radical. *J. Am. Chem. Soc.* **1996**, *118*, 7400–7401. [[CrossRef](#)]
27. Porter, G.; Ward, B. The electronic spectra of phenyl radicals. *Proc. R. Soc. Lond. Ser.-Math. Phys. Sci.* **1965**, *287*, 457–470.
28. Jaquiss, M.T.; Szwarc, M. Reactions of phenyl radicals in solution and in the gaseous phase. *Nature* **1952**, *170*, 312–314. [[CrossRef](#)]
29. Hatton, W.G.; Hacker, N.P.; Kasai, P.H. The photochemistry of nitrosobenzene: Direct observation of the phenyl radical–nitric oxide triplet radical pair in argon at 12 K. *J. Chem. Soc. Chem. Commun.* **1990**, 227–229. [[CrossRef](#)]
30. Scaiano, J.C.; Stewart, L.C. Phenyl radical kinetics. *J. Am. Chem. Soc.* **1983**, *105*, 3609–3614. [[CrossRef](#)]
31. Preidel, M.; Zellner, R. A cw laser absorption study of the reactions of phenyl radicals with NO, NO₂, O₂ and selected organics between 298–404 K. *Ber. Bunsen-Ges. Phys. Chem. Chem. Phys.* **1989**, *93*, 1417–1423. [[CrossRef](#)]
32. Wallington, T.J.; Egsgaard, H.; Nielsen, O.J.; Platz, J.; Sehested, J.; Stein, T. UV–visible spectrum of the phenyl radical and kinetics of its reaction with NO in the gas phase. *Chem. Phys. Lett.* **1998**, *290*, 363–370. [[CrossRef](#)]
33. Cheng, P.Y.; Zhong, D.; Zewail, A.H. Kinetic-energy, femtosecond resolved reaction dynamics. Modes of dissociation (in iodobenzene) from time-velocity correlations. *Chem. Phys. Lett.* **1995**, *237*, 399–405. [[CrossRef](#)]
34. Kadi, M.; Davidsson, J.; Tarnovsky, A.N.; Rasmusson, M.; Akesson, E. Photodissociation of aryl halides in the gas phase studied with femtosecond pump-probe spectroscopy. *Chem. Phys. Lett.* **2001**, *350*, 93–98. [[CrossRef](#)]
35. Alt, H.G. Photochemistry of alkyltransition-metal complexes. *Angew. Chem. Int. Ed.* **1984**, *23*, 766–782. [[CrossRef](#)]
36. Toscano, P.J.; Marzilli, L.G. B12 and related organocobalt chemistry: Formation and cleavage of cobalt carbon bonds. *Prog. Inorg. Chem.* **1984**, *31*, 105–205.
37. Demarteau, J.; Debuigne, A.; Detrembleur, C. Organocobalt complexes as sources of carbon-centered radicals for organic and polymer chemistries. *Chem. Rev.* **2019**, *119*, 6906–6955. [[CrossRef](#)]
38. Bakac, A.; Espenson, J.H. Photochemical generation of alkyl radicals and their reactions with methyl viologen radical cation and with transition-metal complexes in aqueous solution. *Inorg. Chem.* **1989**, *28*, 3901–3904. [[CrossRef](#)]
39. Morandini, F.; Pilloni, G.; Consiglio, G.; Sironi, A.; Moret, M. Cyclopentadienyl and indenyl complexes of rhodium(I) and rhodium(III) containing chiral diphosphines. X-ray structure of (R)c(S)Rh-[(η -5-C₉H₇)Rh(Ph₂PCH(CH₃)CH₂PPh₂)(CH₃)]BPh₄. *Organometallics* **1993**, *12*, 3495–3503. [[CrossRef](#)]
40. Hay-Motherwell, R.S.; Koschmieder, S.U.; Wilkinson, G.; Hussain-Bates, B.; Hursthouse, M.B. Aryl compounds of rhodium: Syntheses and X-ray crystal structures. *J. Chem. Soc. Dalton Trans.* **1991**, 2821–2830. [[CrossRef](#)]
41. Zecchin, S.; Zotti, G.; Pilloni, G. Electrochemistry of coordination compounds: XXII. Electrogeneration and characterization of monomeric iridium(II) organometallic complexes [Ir(R)(CO)(PPh₃)₃]⁺. *J. Organomet. Chem.* **1985**, *294*, 379–388. [[CrossRef](#)]
42. Hetterscheid, D.G.H.; Koekkoek, A.J.J.; Grützmacher, H.; de Bruin, B. The organometallic chemistry of Rh-, Ir-, Pd-, and Pt-based radicals: Higher valent species. *Prog. Inorg. Chem.* **2007**, *55*, 247–347.
43. Fischbach, U.; Rügger, H.; Grützmacher, H. Tris(dibenzo[a,d]cycloheptenyl)phosphane: A bulky monodentate or tetrapodal ligand. *Eur. J. Inorg. Chem.* **2007**, *2007*, 2654–2667. [[CrossRef](#)]

44. Fischbach, U.; Trincado, M.; Grützmacher, H. Oxidative formation of phosphinyl radicals from a trigonal pyramidal terminal phosphide Rh(I) complex, with an unusually long Rh–P bond. *Dalton Trans.* **2017**, *46*, 3443–3448. [[CrossRef](#)]
45. Thaler, E.G.; Foltling, K.; Caulton, K.G. et al. 3-MeC(CH₂PPh₂)₃/rhodium complexes utilize phosphine arm dissociation mechanisms at 25 °C. *J. Am. Chem. Soc.* **1990**, *112*, 2664. [[CrossRef](#)]
46. Boyd, S.E.; Field, L.D.; Hambley, T.W.; Partridge, M.G. Synthesis and characterization of Rh[P(CH₃)₃]₂(CO)CH₃ and Rh[P(CH₃)₃]₂(CO)Ph. *Organometallics* **1993**, *12*, 1720–1724. [[CrossRef](#)]
47. Shafiq, F.; Kramarz, K.W.; Eisenberg, R. Binuclear rhodium alkyl and acyl A-frame complexes: Synthesis, structure and reactivity. *Inorg. Chim. Acta* **1993**, *213*, 111–119. [[CrossRef](#)]
48. Sterenberg, B.T.; Hilts, R.W.; Moro, G.; McDonald, R.; Cowie, M. Heterobinuclear hydrido, alkyl, and related complexes of Rh/Os. Site-specific reductive elimination of methane from a Rh/Os core and the structures of [RhOs(CH₂CN)(CO)₃(dppm)₂] and [RhOs(CH₃)(CO)₃(dppm)₂]. *J. Am. Chem. Soc.* **1995**, *117*, 245–258. [[CrossRef](#)]
49. Antonelli, D.M.; Cowie, M. Unusual, coordinatively unsaturated rhodium/rhenium and iridium/rhenium, alkyl, acyl, and hydrido complexes. Structure of [RhRe(CH₃)(CO)₄(Ph₂PCH₂PPh₂)₂][CF₃SO₃].3CH₂Cl₂. *Organometallics* **1991**, *10*, 2550–2559. [[CrossRef](#)]
50. Anderson, D.J.; Kramarz, K.W.; Eisenberg, R. Synthesis and structure of the diphenyl binuclear rhodium A-frame complex Rh₂(μ-CO)(Ph)₂(dmpm)₂. *Inorg. Chem.* **1996**, *35*, 2688–2691.
51. Addison, A.W.; Rao, T.N.; Reedijk, J.; van Rijn, J.; Verschoor, G.C. Synthesis, structure, and spectroscopic properties of copper(II) compounds containing nitrogen–sulphur donor ligands; the crystal and molecular structure of aqua[1,7-bis(N-methylbenzimidazol-2'-yl)-2,6-dithiaheptane]copper(II) perchlorate. *J. Chem. Soc. Dalton Trans.* **1984**, *7*, 1349–1356. [[CrossRef](#)]
52. Darensbourg, D.J.; Grottsch, G.; Wiegrefe, P.; Rheingold, A.L. Insertion reactions of carbon dioxide with square-planar rhodium alkyl and aryl complexes. *Inorg. Chem.* **1987**, *26*, 3827–3830.
53. Norcott, P.L.; Hammill, C.L.; Noble, B.B.; Robertson, J.C.; Olding, A.; Bissemer, A.C.; Coote, M.L. TEMPO–Me: An electrochemically activated methylating agent. *J. Am. Chem. Soc.* **2019**, *141*, 15450–15455. [[CrossRef](#)]
54. Omelka, L.; Vrabel, I.; Erentova, K.; Dauth, J.; Deubzer, B.; Weis, J. ESR Study of nitroxide radicals generated from triaz-2-en-1-ols. *Helv. Chim. Acta* **1996**, *79*, 663–669. [[CrossRef](#)]
55. Bevington, J.C.; Fridd, P.F.; Tabner, B.J. An electron spin resonance study of some trapped primary radicals. *J. Chem. Soc. Perkin Trans.* **1982**, *2*, 1389–1391. [[CrossRef](#)]
56. Neese, F.; Wennmohs, F.; Becker, U.; Riplinger, C. The ORCA quantum chemistry program package. *J. Chem. Phys.* **2020**, *152*, 224108. [[CrossRef](#)]
57. Kendall, R.A.; Früchtel, H.A. The impact of the resolution of the identity approximate integral method on modern ab initio algorithm development. *Theor. Chem. Acc.* **1997**, *97*, 158–163. [[CrossRef](#)]
58. Neese, F.; Wennmohs, F.; Hansen, A.; Becker, U. Efficient, approximate and parallel Hartree–Fock and hybrid DFT calculations. A ‘chain-of-spheres’ algorithm for the Hartree–Fock exchange. *Chem. Phys.* **2009**, *356*, 98–109. [[CrossRef](#)]
59. Grimme, S.; Antony, J.; Ehrlich, S.; Krieg, H. A consistent and accurate ab initio parametrization of density functional dispersion correction (DFT-D) for the 94 elements H–Pu. *J. Chem. Phys.* **2010**, *132*, 154104. [[CrossRef](#)] [[PubMed](#)]
60. Grimme, S.; Ehrlich, S.; Goerigk, L. Effect of the damping function in dispersion corrected density functional theory. *J. Comput. Chem.* **2011**, *32*, 1456–1465. [[CrossRef](#)]
61. Brandenburg, J.G.; Bannwarth, C.; Hansen, A.; Grimme, S. B97-3c: A revised low-cost variant of the B97-D density functional method. *J. Chem. Phys.* **2018**, *148*, 064104. [[CrossRef](#)] [[PubMed](#)]
62. Zhao, Y.; Truhlar, D.G. Applications and validations of the Minnesota density functionals. *Chem. Phys. Lett.* **2011**, *502*, 1–13. [[CrossRef](#)]
63. Weigend, F.; Ahlrichs, R. Balanced basis sets of split valence, triple zeta valence and quadruple zeta valence quality for H to Rn: Design and assessment of accuracy. *Phys. Chem. Chem. Phys.* **2005**, *7*, 3297–3305. [[CrossRef](#)]
64. Cossi, M.; Rega, N.; Scalmani, G.; Barone, V. Energies, structures, and electronic properties of molecules in solution with the C-PCM solvation model. *J. Comput. Chem.* **2003**, *24*, 669–681. [[CrossRef](#)]